#11530

A MATHEMATICAL MODEL OF DOWNDRAFT EXHAUST HOODS

R.A.Thomas, S.J.Dunnett.

Department of Mathematical Sciences, Loughborough University, Loughborough, Leics. LE11 3TU. U.K.

ABSTRACT

The purpose of the work described in this paper is to develop a mathematical model of downdraft exhaust hoods in order that ways of improving these hoods efficiency can be examined. In this initial study the model developed is two-dimensional. The flow has been assumed to be ideal and the complex potential considered. By use of conformal mappings the airflow in the vicinity of a bench, which is extracting air and also has air being blown down from above, is modelled. Various ratios of extraction to downdraft are considered in order to investigate the most efficient method of operation.

KEYWORDS

Local exhaust, Numerical methods, Computational Fluid Dynamics (C.F.D.), Ventilation efficiency.

INTRODUCTION

Production processes and the emission of noxious gases, vapours, dust or heat often go hand in hand. These emissions affect the state and condition of the air. This could lead to the health and well-being of the workers being harmed, thus creating distressing working conditions and therefore leading to a reduction in the productivity of the company. To combat these problems and maintain the required Health and Safety standards regarding air quality some form of ventilation system is needed to prevent the contaminants from entering the workers breathing zone. The ventilation process removes the contaminated air from the room/building (extract ventilation) and replaces it with clean air (inflow ventilation).

The purpose of a downdraft exhaust hood is to remove the contaminant away from the worker by withdrawing air form below the benchtop in a downward direction. This is usually through a floor grill or a grill in a workbench top. However this style of ventilation often gives unacceptable levels of exposure of the contaminant to the workers within the vicinity. In attempts to improve the efficiency of these hoods air has been blown down from above the hood at a constant rate. This reduced the exposure of the worker but increased the exposure of others working within the area.

The objectives of the theoretical study being undertaken here are to obtain a detailed description of the airflow in the vicinity of the ventilation system. The system considered is a room containing a workbench, through which air is extracted in a downward direction. Directly above the bench, in the roof of the physical domain, is an opening through which air is blown, see figure 1.It is also assumed that there is a crossdraft airflow of velocity, v_c, in the room containing the ventilation system. In this paper the airflow in the vicinity of the workbench has been considered. The model has been developed by considering crossdraft and downdraft situations separately and then combining the results for the complete model. Figures 1a, b and c shows the cases of (a) crossdraft airflow only, (b) downdraft airflow plus extraction of airflow through the bench and (c) both crossdraft and downdraft airflows combined with extraction through the bench.

$$M = \frac{h}{\pi}\int_1^a f(\varsigma)d\varsigma \qquad (9(a))$$

$$L = \frac{h}{\pi}\int_a^b f(\varsigma)d\varsigma \qquad (9(b))$$

Equations (9) cannot be solved analytically. In order to determine a and b the function:

$$f(a,b) = \left[\frac{h}{\pi}\int_1^{\sqrt{a-1}} f(\eta)d\eta - M\right]^2 + \left[\frac{h}{\pi}\int_1^{\sqrt{b-1}} f(\eta)d\eta - (L+M)\right]^2 \qquad (10)$$

where $\eta^2 = \varsigma - 1$

was minimised. This was achieved using a NAG library routine (E04CCF), where the integrals where replaced with the approximation given by the Extended Simpsons Rule (Press (1992)).

Once the co-ordinates in the ς-plane corresponding to the corners of the workbench in the physical z-plane had been obtained then the next step was to find the full set of ς co-ordinates corresponding to all the points in the physical plane. The flow velocities at those points could them be determined and the flow field investigated. The axes are set in the physical plane, z-plane, with the point D being located at the origin. Equation (7) can be inverted and expressed in finite difference form as:

$$\varsigma_{i+1} = \varsigma_i + \frac{\Delta z \pi \varsigma_i}{h}\sqrt{\frac{(\varsigma_i - 1)(\varsigma_i - ab)}{(\varsigma_i - a)(\varsigma_i - b)}} \qquad (11)$$

where Δz = step in the z-direction
$= \Delta x + i\Delta y$

Hence taking a mesh in the z-plane with step Δx, Δy the corresponding values of ς were obtained from equation (11).

The velocities are given by equation (4) with K and c given by equations (5) and (6) respectively. Hence equation (4) becomes:

$$\frac{dw}{dz} = U\sqrt{\frac{(\varsigma - 1)(\varsigma - ab)}{(\varsigma - a)(\varsigma - b)}} \qquad (12)$$

i.e.:

$$u - iv = U\sqrt{\frac{(\varsigma - 1)(\varsigma - ab)}{(\varsigma - a)(\varsigma - b)}} \qquad (13)$$

Once the velocity components, u and v, had been determined the velocity vectors were plotted using SIGMAPLOT version 2.01, a scientific graphics package.

Downdraft

Figure 3a shows the set up being considered for the downdraft airflow in full detail. The sink in the workbench at R takes in (Nx100) % of the air. Since the situation is symmetrical, the sinks at C∞ and H∞ exhaust the same amount of air, this will be given by ((1–N)/2)x100 %.

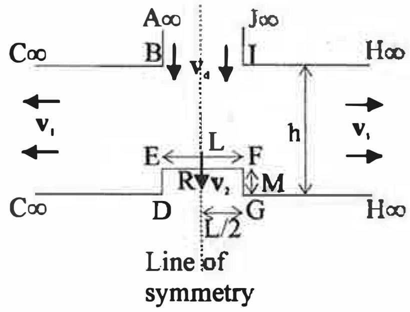

Figure 3a. Diagrammatic representation of the physical plane for the downdraft model.

Due to the symmetry of the physical z-plane, in this case it can be transformed into the computational ς-plane, as shown in figure 3b.

Figure 3b. Diagrammatic representation of the ς-plane for the downdraft model.

The Schwarz-Christoffel transformation is:

$$\frac{dz}{d\varsigma}=\frac{K}{(\varsigma-b)(\varsigma+b)}\times\sqrt{\frac{(\varsigma-c)(\varsigma+c)(\varsigma-1)(\varsigma+1)}{(\varsigma-a)(\varsigma+a)}} \tag{14}$$

Thus there are four unknowns: a, b, c, and K. The sink at R takes in the fraction N of the total flux, i.e.:

$$Q_R=NQ \tag{15}$$

where Q = total flux.
Q_R = flux at R.
N = fraction of air extracted at R.

because of the symmetry of the situation:

$$Q_{C\infty}=Q_{H\infty}=\frac{1-N}{2}Q \tag{16}$$

where $Q_{C\infty}$ = Flux at C∞
$Q_{H\infty}$ = Flux at H∞

Thus the complex potential is given by:

$$w=\frac{(1-N)Q}{2}\ln(\varsigma+b)+\frac{NQ}{2}\ln\varsigma+\frac{(1-N)}{2}\ln(\varsigma-b) \tag{17}$$

dw/dz was obtained from equations (14) and (17) using:

$$\frac{dw}{dz}=\frac{dw}{d\varsigma}\frac{d\varsigma}{dz} \tag{18}$$

From conditions at H∞ and at J∞ two expressions were obtained for K, i.e.:

$$K=\frac{2hb}{\pi}\sqrt{\frac{(b-a)(b+a)}{(b-c)(b+c)(b-1)(b+1)}} \tag{19}$$

and:

$$K=i\frac{L}{\pi} \tag{20}$$

Combining equations (19) and (20) results in the condition:

$$a^2=\frac{b^2(\alpha^2+1)-(c^2+1)+c^2/b^2}{\alpha^2} \tag{21}$$

where α = 2h/L=constant.

It can also be shown that:

$$b(1+\alpha^2)^{1/2}>c \tag{22}$$

The problem has now been reduced to finding two unknowns b and c. To find these two unknowns two lengths were required. The method of solution used was different to that used in the solution of crossdraft model. Initial guesses b* and c* were made for b and c, these where then used to calculate approximations l_1 and l_2 to the physical lengths L_1 and L_2. The guesses b* and c* were then altered slightly to give new lengths and an iterative process followed until $|L_1-l_1|$ and $|L_2-l_2|$ were less than a given tolerance level, these values of b* and c* are then the required values for b and c.

Once b and c were determined, and hence a from equation (21), the finite difference scheme was employed to determine the corresponding points in the ς-plane for a mesh of points in the z-plane, as in the crossdraft model. Once the points were determined the velocity components u and v in the z-plane could be determined as in the crossdraft model. The downdraft velocity $\mathbf{v_d}$ was taken to be (0.0,-2.0) ms^{-1} as an experimental study by J.Eloranta et. al.

(1993) regarding ventilation for welding and soldering processes had velocities in the range (0.0,-2.6) ms^{-1} and (0.0,-2.3) ms^{-1} being emitted from the opening. Various values of N were considered. The airflow pattern was plotted using SIGMAPLOT.

Full Model

To create the complete model (see figure 1c), which combines the crossdraft and downdraft, the data from the two models for crossdraft and downdraft airflows were combined and the velocities added to give the new velocities

COMPUTATIONAL METHOD

Using the C.F.D. package FLUENT (version 4.32) a computational model of the physical plane was made. The set up modelled was that which combined the crossdraft and downdraft airflows. The Reynolds number for the model at room temperature was very large $\approx 8.6\times10^4$. Currently the model being examined is laminar, however it is intended to extend this to a turbulent model.

The differences between the computational model and the numerical model are few, the outlet in the workbench is now of a finite length (L/3=0.1m) and is defined to be an inlet with a negative v-velocity rather than an outlet. This is because the velocity at this point can be determined via the conservation of flux.

Using FLUENT an irregular grid was set up to cover the physical plane with a finer mesh being placed over the areas of greatest interest. The main concentration of cells was around the workbench and its step and also around the ceiling inlet. The cell distribution was then weighted to give a smooth grid. The convergence criterion used was FLUENT's own, this is when the sum of the residuals for the pressure, u and v velocities is less than 1×10^{-3}. As with the numerical model varying values of N where examined.

NUMERICAL RESULTS

Results were obtained for various situations, in particular for various values of N where N is the ratio of the amount of air extracted to the amount of air blown down from above. As expected it was found that the lower the suction rate the more influence the crossdraft had on the airflow pattern.

In figure 4a the airflow pattern is shown when there is a crossdraft airflow with no downdraft there are two outlets, one in the workbench and air is being extracted through the bench. In the figure half the total amount of air is exhausted through the bench. In the figure the velocity vectors are shown, the lengths of the vectors are proportional to the magnitude of the velocity and the magnitudes are evaluated at the midpoints of the vectors. As can be seen in the figure close to the workbench the air is being pulled into the extraction system, hence extracting any contaminant in that region. Away from the bench the crossdraft is carrying the clean air across the room..

In figure 4b the velocity vectors are shown for when there are both crossdraft and downdraft airflows present with N=1/2, i.e. half the amount of air is extracted as is blown down from above. The downdraft velocity, $\mathbf{v_d}$, is much larger than that of the crossdraft, $\mathbf{v_c}$, and as can be seen this velocity has a greater effect on the air motion than that of the crossdraft.

Comparing figures 4a and 4b it can be seen that the effect of including a downdraft airflow is to blow the air downwards and therefore away from the workers breathing zone. However the downdraft velocity also results in the airflow, close to the left hand side of the bench, moving away from the bench and hence the worker. This could result in contaminant being carried to other people working within the vicinity, as has been found in working situations. Other values of extraction and downdraft rates have been considered and the same behaviour observed. The results obtained are for a constant velocity across the opening BI, see figure 3a. It is possible that taking a variable velocity may reduce the problems of increasing the exposure of other people in the vicinity. It is planned to investigate this in the future.

COMPUTATIONAL RESULTS

The computational results showed that for the full model the lower the suction rate through the workbench then the greater influence the crossdraft had on the motion of the airplume from the downdraft, as in the numerical model. They have also showed small regions of recirculation around the edges of the workbench where air is being pulled up from the workbench surface and into the air flowing towards the outlet.

DISCUSSION

Both the numerical and computational methods used for the full model showed that the smaller the suction ratio through the workbench the more effect the crossdraft had on the airflow created by the downdraft.

Form the laminar model it can be seen that there is an area of recirculation behind the bench. This recirculation will never be modelled by the ideal flow model developed here, however this may not be the main area of contaminant for a person as it is not in the direct line of their breathing zone. The potential model developed here makes it possible to investigate the general flow behaviour in the vicinity of the ventilation system easily and efficiently. It requires a fraction of the computational resources required in solving the laminar flow model. Using this potential model the effects of different mechanisms, i.e. downdraft, air extraction can be investigated. However if a detailed description of the airflow was required particularly in the wake of the bench, other models, such as C.F.D. models need to be adopted.

ACKNOWLEDGEMENTS

We would like to acknowledge the following people for their help: Prof. Derek Ingham (University of Leeds), Philip Trevelyan (Research student, University of Leeds) and Prof. Gwynne Evans (De Montfort University).

Thank you to EPSRC and Bernard Fletcher of the Health and Safety Laboratories, Sheffield, U.K. for the funding of this project.

REFERENCES

Eloranta, J., Schimberg, R.W., Hyvärinen, M., Rautio, S., Welling, I. (1993) *Uses of Local Ventilation in Welding and Soldering Processes.* Ventilation '91. ACHIH 1993.

Heinsohn, R.J. (1991) *Industrial Ventilation Principles.* John Wiley & Sons, Chichester, U.K.

Milne-Thompson. (1968) *Theoretical Hydrodynamics.* Macmillian

Press, W.H., Teukolsky, S.A., Vettering, W.T., Flannery, B.P. (1992) *Numerical Recipes in Fortran.* Cambridge University Press, Cambridge, U.K.

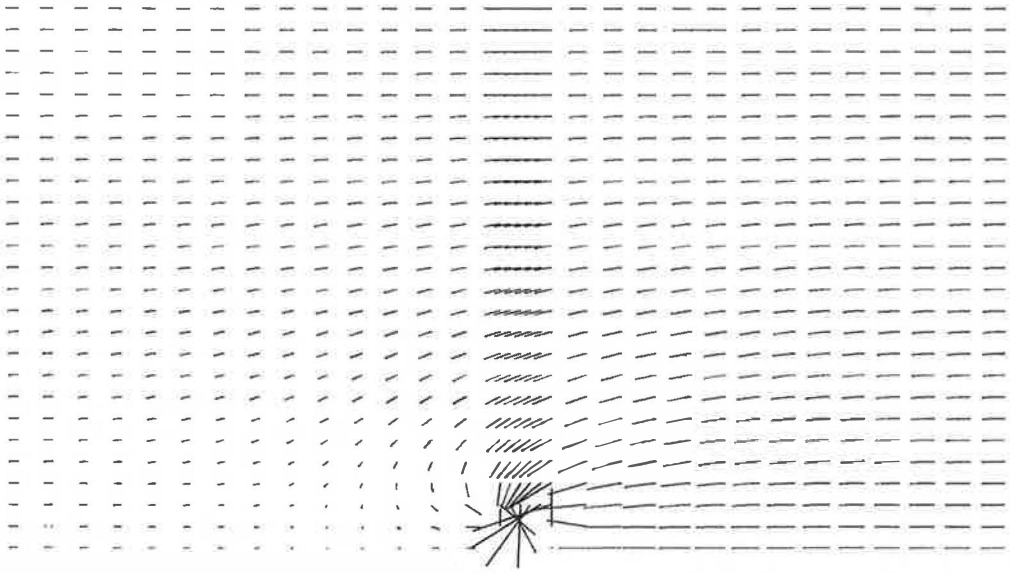

Figure 4a. Graphical representation of the velocity vectors when there is a crossdraft airflow present.
Half the air is extracted through the workbench.

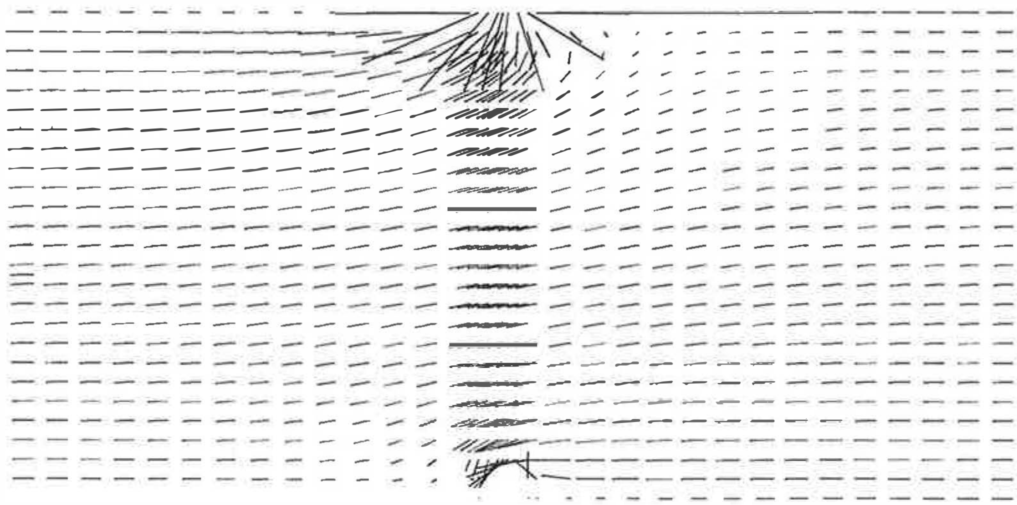

Figure 4b. Graphical representation of the velocity vectors when there are crossdraft and downdraft airflows present, N=1/2.